

Operational mode and gas species effects on rotational drag in pneumatic dead weight pressure gauges

James W Schmidt, Bernard E Welch and Charles D Ehrlich

Thermophysics Division, National Institute of Standards and Technology, Gaithersburg, Maryland 20899, USA

Received 28 February 1992, in final form 29 June 1992, accepted for publication 7 September 1992

Abstract. Rotational dissipation in a low-pressure pneumatic dead weight piston gauge has been measured for four gases: He, H₂, N₂ and SF₆. Significant differences in the rotational dissipation were observed between the four gas species. Even larger differences were observed between two operational modes (gauge and absolute). The measured results are interpreted by a model for the rotational dissipation due to the gas in the annular region between the piston and cylinder. Good agreement was found between the measured and modelled results for all four gas species with essentially no adjustable parameters.

Nomenclature

A	Area of overlap between piston and cylinder	v_ϕ	Flow velocity of a fluid element in the azimuthal direction
b_1	$4\eta kT/(M\bar{c}h)$	v_r	Radial component of molecular velocity
b_2	$64\eta kT/(\pi M\bar{c}h)$	z	Axial coordinate
\bar{c}	Mean molecular speed of the pressurizing gas	z_0	Axial coordinate (top of piston)
D	$\pi h^3 R_1/6$	z_1	Axial coordinate (bottom of piston)
F_1	Momentum transfer function (angular direction)	Γ_{an}	Angular torque coefficient (due to gas in the annulus)
F_2	Momentum transfer function (axial direction)	Γ_s	Angular torque coefficient (due to gas in bell jar)
F_ϕ	Drag force on the piston in the azimuthal direction	Γ	Angular torque coefficient (all sources)
H_i	Clearances of various weights loading piston	λ	Mean free path between intermolecular collisions
h	Crevice width	Λ	Mean distance between molecular collision events (with walls or other molecules)
I	Moment of inertia of piston and weights	η	Viscosity of pressurizing gas
J	Molecular flow rate (number of molecules/unit time/unit area)	η_{air}	Viscosity of the gas in the bell jar
k	Boltzmann's constant	θ	Angular variable of integration
M	Molecular mass of the pressurizing gas	τ	Rotational period of piston assembly
L	Length of the region of overlap (piston and cylinder)	τ_0	Rotational period of piston assembly at initial time
n	Number density of gas molecules	Ω	Angular frequency of piston assembly
P	Pressure variable	Ω_0	Angular frequency of piston assembly at initial time
P_0	Pressure at top of piston	$d\Omega/dt$	Angular deceleration of the piston assembly
P_1	Pressure at bottom of piston		
r	Radial variable		
R_1	Radius of the piston		
R_2	Radius of the cylinder		
R_i	Radii of various weights loading piston		
t	Time		
t_0	Mean times between intermolecular collisions		
t_1	Mean times between collisions with walls of the crevice		
T	Temperature (in K)		

1. Introduction

The physical dimensions of modern dead weight piston gauges can be manufactured to within very close tolerances ($\pm 0.1 \mu\text{m}$ or better). With these gauges, pressures

can be generated and/or measured reproducibly to within a few parts per million (ppm) [1–3]. Recently, two effects have been observed in some gauges to be greater than had been previously assumed for pneumatic gauges [4, 5]. One effect is the gas species effect which, as the term implies, is observed when a gauge pressurized with one species of gas generates a pressure that differs from the pressure generated using a second species for the same mass load. While this effect is usually small, it is larger than the resolution of the best gauges available. A second effect is the gauge mode to absolute mode effect and, as the terms imply, is observed when the pressures generated by the same gauge in the two different modes of operation differ by an amount slightly different than the ambient atmospheric pressure.

Since the two effects are almost certainly related to the flow of gas through the annular region between the piston and cylinder, another property that depends on details of the physics of the gas or fluid in the annular region was measured. This property is the rotational deceleration $d\Omega/dt$ of a piston assembly with known moments of inertia inside a close fitting cylinder [1]. The dependence of the rotational deceleration on gas species arises primarily from the viscosity difference between gases. All else being equal, a more viscous gas produces more dissipation. However, this dependence on gas species is somewhat more complicated because the viscosity (or more precisely the momentum transfer coefficient) of the gas in the crevice depends on the ratio λ/h , where λ is the mean free path of a gas atom or molecule and h is the crevice width. In some cases a gas with a higher viscosity but with a smaller molecular size and hence a larger ratio will provide less dissipation than another gas with a smaller viscosity. In addition very different pressure profiles along the length of the crevice can result from a change of gas species.

In the next section a model will be developed for the momentum transfer function in the crevice. The functional dependence on pressure and gas species will be given and to complete the model the pressure profile along the length of the crevice will also be developed. The model contains essentially no adjustable parameters although in the analysis of the present measurements we first used the crevice width as a parameter to obtain the best fits to the data for each gas, but then used the average value for the final analysis.

In section 3 data in the form of spin period against time will be presented. Data were obtained from four different gases including helium (He), nitrogen (N_2), sulphurhexafluoride (SF_6) and hydrogen (H_2). The present model will then be compared with the data in section 4.

2. Theory

The rotational motion of the piston assembly is described by the following differential equation:

$$I d\Omega/dt \approx -\Gamma\Omega \quad (1)$$

where $\Gamma = \Gamma_{an} + \Gamma_s$ is considered to be the angular torque coefficient arising from two sources, the drag due to the gas in the annular region Γ_{an} and the aerodynamic drag due to the gas in the bell jar on all of the other moving surfaces Γ_s . All other sources were considered to be negligible in comparison with these two. In equation (1) Ω is the angular frequency, I is the moment of inertia and $I d\Omega/dt$ is the change in angular momentum per unit time due to the deceleration torque ($-\Gamma\Omega$) acting on the piston assembly. The solution to equation (1) is $\Omega = \Omega_0 \exp(-\Gamma t/I)$ or, equivalently, $\tau = \tau_0 \exp(+\Gamma t/I)$ where τ is the period, which is the quantity actually measured in these experiments.

Estimates of the coefficients Γ_{an} and Γ_s show that the larger contribution to Γ is Γ_{an} due to the gas in the annular region and that Γ_s is typically a few per cent of Γ_{an} in gauge mode and is less than 1% in absolute mode. Γ_{an} is given by the following equation for two limiting cases corresponding to the viscous flow regime [6] and the collisionless molecular flow regime respectively [7, 8].

$$\Gamma_{an} \approx \frac{R_1^2 A}{h} \begin{cases} \eta & \lambda/h \ll 1 \\ M\bar{c}Ph/4kT & \lambda/h \gg 1. \end{cases} \quad (2a)$$

$$(2b)$$

Here R_1 is the radius of the piston, h is the annular width or radial clearance between piston and cylinder, A is the cylindrical surface area of the piston within the cylinder, η is the viscosity of the gas, M is the molecular mass, P is the pressure, \bar{c} is the mean molecular speed ($= (8kT/\pi M)^{1/2}$), k is Boltzmann's constant, T is the temperature in Kelvin and λ is the mean free path of the gas molecules. (See the appendix for derivations of equations (2a) and (2b).)

In the gauge mode of operation the mean free path of the gas molecules λ is typically smaller than the annular width h everywhere in the annulus and so this physical situation should approach that described by equation (2a). In the absolute mode of operation $\lambda/h \ll 1$ at the bottom of the piston, but at the top of the piston (vacuum) $\lambda/h \gg 1$ and therefore there is a region where equation (2b) applies. Instead of using equations (2a) and (2b) separately, we now obtain an effective viscosity or momentum transfer function $F_1(\lambda/h)$ that bridges the two limiting cases indicated by these equations. $F_1(\lambda/h)$ should equal $M\bar{c}Ph/4kT$ at low pressures where $\lambda/h \gg 1$ and it should approach the gas viscosity η asymptotically for large P where $\lambda/h \ll 1$. The functional form [9–11] of the momentum transfer function $F_1(x)$ can be obtained by noting that, as an effective viscosity, it should be proportional to the number density of molecules $n(= P/kT)$, the molecular mass M , the mean molecular speed \bar{c} , and a length $\Lambda = \bar{c}t$ which represents the mean distance that a molecule travels in time t before undergoing a collision event either with another molecule or with the walls, i.e.

$$F_1 \propto nM\bar{c}\Lambda. \quad (3)$$

In the higher pressure viscous flow regime, Λ is equal to the molecular mean free path $\lambda \approx \bar{c}t_0$, while in the

low-pressure molecular flow regime in which $\lambda/h \gg 1$ the length Λ must be of the order of $h \approx \bar{c}t_1$. t_0 and t_1 define the mean times between collision events in the two regimes. Following Reif [10], we note that the total probability per unit time ($1/t$) that a given molecule undergoes a collision event is the sum of the individual probabilities for the two types of events, i.e. a collision with another molecule or collision with the walls of the annulus:

$$\left(\frac{1}{t}\right) = \left(\frac{1}{t_0}\right) + \left(\frac{1}{t_1}\right). \quad (4)$$

By substituting for t , t_0 , and t_1 in terms of Λ , λ and h respectively and solving for Λ one obtains

$$\Lambda \approx \frac{\lambda}{1 + \lambda/h}. \quad (5)$$

Substituting this expression for Λ into equation (3) yields the approximate functional form for F_1 :

$$F_1 \propto \frac{nM\bar{c}\lambda}{1 + \lambda/h}. \quad (6)$$

F_1 is defined to be:

$$F_1(P) \equiv \left(\frac{\eta}{1 + b_1/P}\right) \quad (7)$$

where

$$\frac{b_1}{P} = \frac{4\eta kT}{McPh} \quad (8a)$$

$$\approx \frac{\lambda}{h} \quad (8b)$$

The factor $\eta (\approx M\bar{c}n\lambda/3)$ in equation (7) ensures an asymptotic approach to η in equation (2a) in the limit $\lambda/h \ll 1$. The definition of b_1 in equation (8a) ensures a smooth match onto $M\bar{c}Ph/4kT$ in equation (2b) in the limit $\lambda/h \gg 1$. Although not done here, it is often the practice with the equations describing spinning rotor gauges, which equation (2b) parallels, to include an accommodation coefficient in the expression for b_1/P to account for differences between species [7, 12].

The momentum transfer function $F_1(P)$ will now be used to calculate Γ_{an} . One starts by writing down the elemental contribution to Γ_{an} arising from an elemental piston-cylinder overlap area $dA = 2\pi R_1 dz$ due to gas in the annular region at pressure P :

$$d\Gamma_{an} = \frac{R_1^2}{h} F_1(P) dA. \quad (9)$$

This equation, when integrated over the overlap region, will supersede equations (2a) and (2b). Equation (9) can be integrated provided one can obtain the pressure profile $P(z)$ in terms of the axial distance z along the annular region from the top to the bottom of the piston.

To calculate the dependence of P (and hence F_1) on z , it is observed that under steady state conditions the net flow of molecules must be constant in the axial direction z in the annular region [11, 13]. The molecular

flow rate (number of molecules per unit time) through an annulus of radial dimensions R_1 and $R_1 + h$ and of length Δz in the viscous flow regime is given by the equation [14, 15]

$$J \approx \frac{\pi h^3 n R_1}{6\eta} \frac{\Delta P}{\Delta z} \quad (10)$$

and the molecular flow rate through an annulus in the molecular flow regime is [16, 17]

$$J \approx \frac{4\pi\bar{c}h^2 R_1}{3kT} \frac{\Delta P}{\Delta z}. \quad (11)$$

One can represent J in both regimes by the single equation:

$$J = D(n/F_2) dP/dz \quad (12)$$

where F_2 represents a second momentum transfer function which is taken as:

$$F_2(P) = \left(\frac{\eta}{1 + b_2/P}\right). \quad (13)$$

The choice of $D = \pi h^3 R_1/6$ and $b_2 = 64\eta kT/\pi Mch$ ensures that equation (12) will match smoothly onto equations (10) and (11), which represent the bottom and the top of the annulus respectively. The functional form of (13) has been chosen in the same spirit as that of F_1 earlier in the text. Next (12) is integrated from the top of the piston z_0 at reference pressure P_0 to an arbitrary position z at pressure P with $n = P/kT$. This yields:

$$z - z_0 = \frac{D}{J\eta kT} \int_{P_0}^P P \left(1 + \frac{b_2}{P}\right) dP. \quad (14a)$$

$$= \frac{D}{J\eta kT} [(P^2 - P_0^2)/2 + b_2(P - P_0)]. \quad (14b)$$

The above quadratic equation is solved for $P(z)$ and the physically meaningful 'positive' root is taken to obtain the pressure profile $P(z)$:

$$P(z) =$$

$$-b_2 + \left(b_2^2 + 2 \left[P_0^2/2 + b_2 P_0 + \frac{J\eta kT}{D} (z - z_0) \right] \right)^{1/2}. \quad (15)$$

Also note that J can be evaluated for a given set of conditions P_0 , P_1 , T and η :

$$J = D[(P_1^2 - P_0^2)/2 + b_2(P_1 - P_0)]/\eta kTL \quad (16)$$

where P_1 is the system pressure at the bottom of the piston z_1 and $L = z_1 - z_0$. Equations (15) and (16) define a pressure profile in the annulus and exhibit the pressure profile's dependence on gas species and pressures P_0 and P_1 . Figure 1 exhibits an example of the pressure profile's dependence on gas species in both gauge and absolute modes. In all of the above discussion we have assumed h to be independent of position z . For a discussion of how a variation of h with z may influence the pressure profile the reader is referred to the work of Bass [18].

Returning now to equation (9), one can integrate it

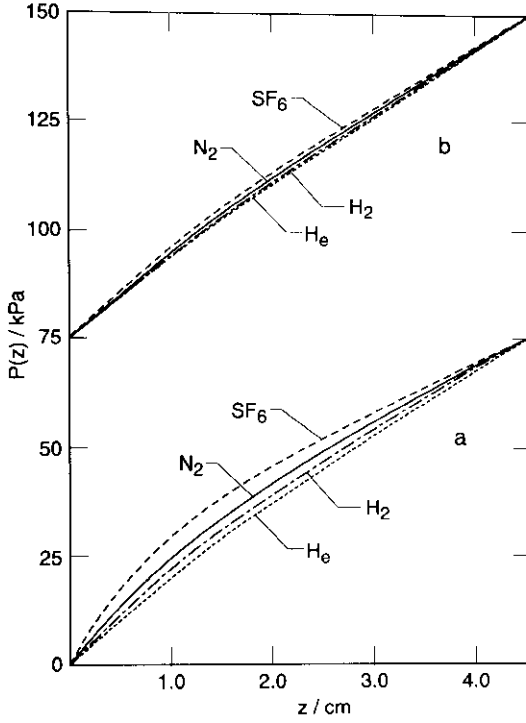


Figure 1. Model pressure profile $P(z)$ against vertical distance from top ($z = 0$) to bottom ($z = 4.5$ cm) of the piston for four gases N_2 , He , SF_6 and H_2 . Both absolute (a) and gauge (b) modes are displayed with an applied pressure difference in each case ≈ 75.0 kPa. The model is for NIST piston gauge PG36 and assumes a mean radial clearance $h = 1.61 \mu\text{m}$. The gas species effect is clearly visible here in the absolute mode.

using the above pressure profile to obtain Γ_{an} :

$$\Gamma_{\text{an}} = \frac{R_1^2}{h} \int_0^{2\pi} R_1 d\theta \int_{z_0}^{z_1} F_1[P(z)] dz \quad (17a)$$

(change the variable of integration from z to P via equation (14b))

$$= \frac{2\pi R_1^3}{h} \int_{P_0}^{P_1} F_1(P) \frac{D}{J\eta kT} (P + b_2) dP \quad (17b)$$

$$= \frac{2\pi R_1^3}{h} \frac{D}{J\eta kT} \int_{P_0}^{P_1} \frac{\eta}{1 + b_1/P} (P + b_2) dP \quad (17c)$$

$$= \frac{2\pi R_1^3}{h} \frac{D}{JkT} \left\{ \frac{(P_1^2 - P_0^2)}{2} + (b_2 - b_1) \right. \\ \left. \times \left[(P_1 - P_0) - b_1 \log \left(\frac{P_1 + b_1}{P_0 + b_1} \right) \right] \right\} \quad (17d)$$

(and substitute for J using equation (16) and simplify to get):

$$= \frac{2\pi R_1^3}{h} \eta L \left\{ 1 + 2 \left(\frac{b_2 - b_1}{P_1 + P_0} \right) \right. \\ \left. \times \left[1 - \frac{b_1}{P_1 - P_0} \log \left(\frac{P_1 + b_1}{P_0 + b_1} \right) \right] \right\} \left/ \left(1 + \frac{2b_2}{P_1 + P_0} \right) \right. \quad (17e)$$

Equation (17e) now supersedes equations (2a) and

(2b) and will be used as a basis to interpret the wide variation (by a factor of eight) in measured values of Γ . The gas species enters into the rotational dynamics as indicated in equation (17e) through the viscosity η and the molecular mass M used in the definitions of b_1 and b_2 . Figure 2 clearly shows differences in the momentum transfer function $F_1[P(z)]$ plotted as a function of z for the four cases N_2 , He , SF_6 and H_2 in absolute mode. A description of how measured values of Γ are obtained is given in section 3. Values calculated by the model described above will then be compared with these measured values.

3. Measurements

Spin time measurements were made using one of the three pistons of the three piston gauge apparatus (TPGA) which is currently under development to investigate the gas species and operational mode effects in further detail. The TPGA is shown schematically in figure 3. The middle piston gauge (number 2) is the gauge under investigation and gauges 1 and 3 can be used to generate and measure accurately the applied pressure and the reference back pressure, respectively, of gauge 2. This design makes it possible to operate gauge 2 in a mode intermediate between the conventional 'absolute' and 'gauge' modes. Due to the long spin times involved in the present measurements, it was necessary to automate the height control for gauge 2. A metering valve was used to bleed in more gas than escaped through the annular region and an automotive fuel injector [19] was used to remove any excess. To control the height of gauge 2 the injector was used with feedback from an inductive position sensor, a digital voltmeter and a microcomputer. The position sensor on gauge 2 was able to detect rotational motion as well as vertical position of the piston. For

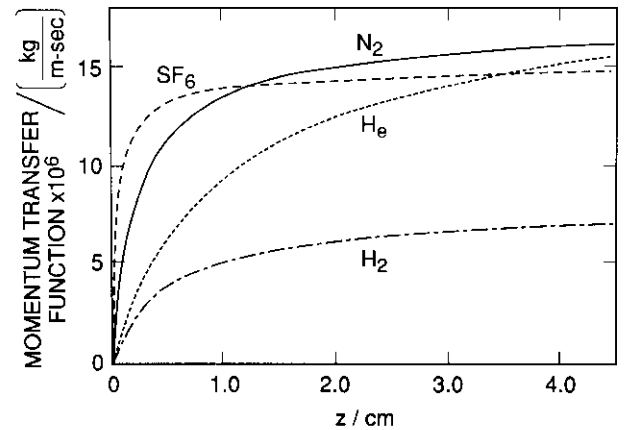


Figure 2. Momentum transfer function $F_1(z)$ against vertical distance from top to bottom of the piston for four gases N_2 , He , SF_6 and H_2 . The absolute mode is displayed here with an applied pressure difference in each case ≈ 75.0 kPa. The model is for NIST piston gauge PG36 and assumes a mean radial clearance $h = 1.61 \mu\text{m}$. The gas species effect is clearly visible here.

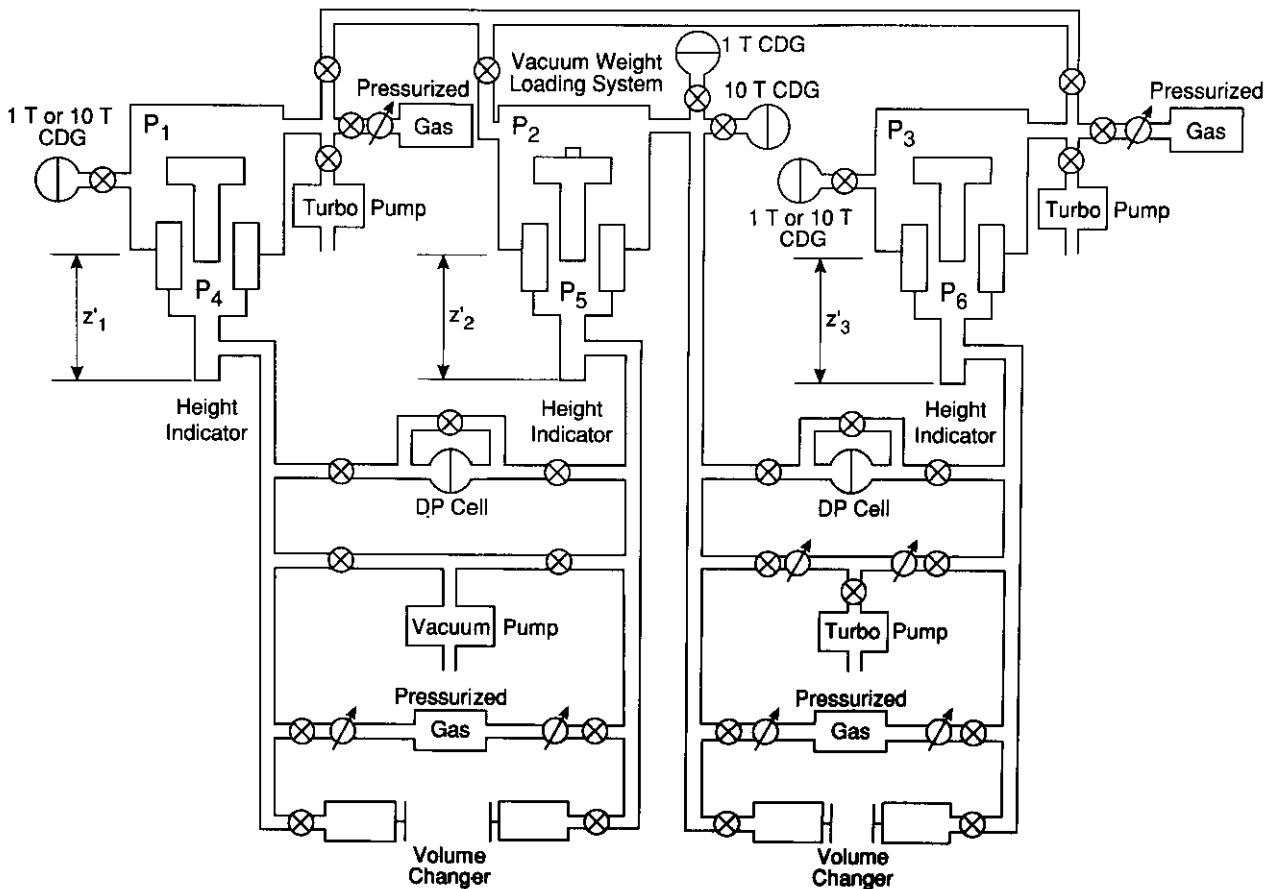


Figure 3. Schematic drawing of the NIST three piston gauge apparatus (TPGA) under development to investigate gas species effects and gauge mode to absolute mode effects. The middle piston gauge is under investigation. The piston gauge on the left measures applied pressure, the one on the right the reference pressure.

the experiments described here it was only necessary to know the nominal pressure being generated by gauge 2, so that gauges 1 and 3 were usually isolated from the system.

The piston gauge used in the 2 position and on which spin time measurements were made is denoted as PG36, and is a commercial gas operated, gas lubricated gauge with a hollow stainless steel piston and a tungsten carbide cylinder with a nominal effective area of $3.356 \times 10^{-4} \text{ m}^2$ and a nominal radial clearance of $1.5 \pm 0.5 \mu\text{m}$. This gauge was examined under a variety of operating conditions. Four gases, nitrogen, helium, sulphurhexafluoride and hydrogen, were alternately used to float the piston. Three moments of inertia corresponding to three different mass loads (pressure differences) spanning one order of magnitude were used in the measurements. In addition, the gauge was operated in both the gauge and absolute modes. A few data points were taken with reference pressure $P_0 \approx 50 \text{ kPa}$.

Some typical spin time data are displayed in figures 4 and 5 in which $\ln(\tau)$ is plotted against time. In each of these figures the clock was arbitrarily set to zero when the period τ equalled 1 s. Thus the slopes (Γ/I) of the lines representing various conditions can be readily compared. The data plotted in figure 4 display the kinematic effect that an object with a larger moment spins proportionately longer, as it should. Figure 5

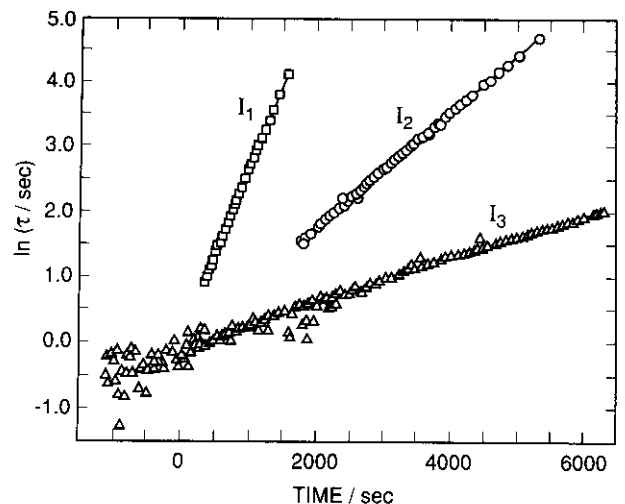


Figure 4. Natural logarithm of the rotation period τ against time for PG36 using three moments of inertia in gauge mode: $I_1 = 0.00114 \text{ kg m}^2$; $I_2 = 0.00389 \text{ kg m}^2$; and $I_3 = 0.0121 \text{ kg m}^2$. The pressurizing gas was N_2 . The slopes of the lines are a measure of Γ/I . The timer was arbitrarily set to zero when the period was 1 s or $\ln(\tau/\text{s}) = 0.00$.

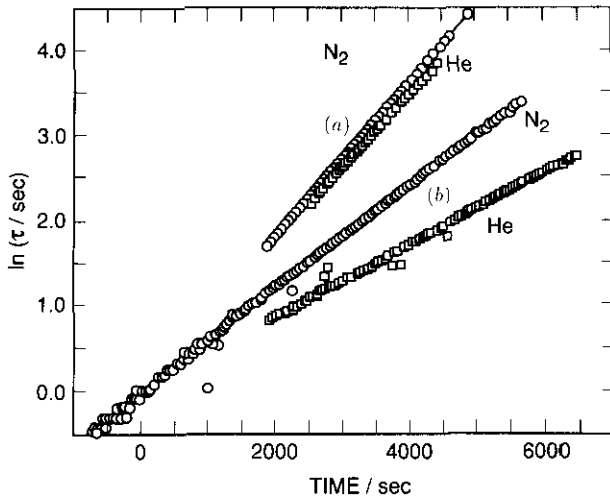


Figure 5. Natural logarithm of the rotation period τ against time for two gases N_2 and He. Each gas was used in both gauge (a) and absolute (b) modes. The same moment of inertia ($I = 0.00389 \text{ kg m}^2$) was used in each case shown.

shows the gauge mode to absolute mode effect and the gas species effect for He and N_2 (for the same mass load and moment of inertia). Data for H_2 and SF_6 have been left off of this figure for clarity but are displayed in figures 6(c) and 6(d) in the form of Γ against generated pressure. In all, more than 100 runs were made under various conditions as described above. The measured values of Γ are plotted in figures 6(a)–6(d) against applied pressure.

4. Discussion

As can be seen in figures 6(a)–6(d), Γ is not very dependent on pressure in the gauge mode. Of the two modes of operation, the gauge mode corresponds more closely to a simple viscous flow model of the fluid or gas in the annular region, where λ is shorter than h over the length of the annular region. In the simple viscous flow model, viscosity (and hence Γ) is independent of pressure as shown by the dotted lines in figures 6(a)–6(d). Although the gauge mode results correspond approximately to the simple viscous flow model, there is some deviation from the simple viscous flow model for some gases at lower pressures, and this is predicted by the present model (full line). The present model for Γ_{an} (equation (17e)) shows a slight decrease as differential pressure ($P_1 - P_0$) is decreased. In the gauge mode (as can be seen when comparing figures 6(a)–6(c)), Γ_{an} is weakly dependent on the gas species. H_2 is an exception (figure 6(d)) and reflects the fact that it has a viscosity which is only half that of N_2 , He, and SF_6 as indicated in table 1.

The most striking effects observed in the present measurements are the changes in Γ in going from the gauge mode to the absolute mode and in changing the applied pressure in the absolute mode. The effect is most

pronounced in He and H_2 but can be seen clearly in each of figures 6(a)–6(d).

In order to model our results we first estimated Γ_s from dimensional measurements of the weight stack and clearances between the various rotating and stationary elements of the gauge, i.e. $\Gamma_s \propto \eta_{air} \sum R_i^3 / H_i$, where η_{air} is the effective viscosity of the gas in the bell jar surrounding the piston and cylinder, R_i are the various radii of the weights and H_i are the various clearances between the rotating weights and the stationary surroundings. Obviously the largest contributions to Γ_s occurred where the clearances H_i were smallest and/or the diameters of the weights were largest. For the present system the smallest clearances occurred between the bell jar covering the gauge and the largest diameter weights in the stack. Estimates were obtained for $\Gamma_s \approx (0.10, 0.20, 0.37 \pm 0.5) \times 10^{-6} \text{ kg m}^2 \text{ s}^{-1}$ respectively for the smallest to the largest of the three weight stacks used. Γ_s was set equal to zero for each of the three weight stacks in the absolute mode since in this case η_{air} is close to zero.

The fitted results from the present model $\Gamma(h) = \Gamma_{an}(h) + \Gamma_s$ are displayed as full lines and broken curves (gauge and absolute modes respectively) in figures 6(a)–6(d). A least-squares fitting algorithm first found the value of h that generated the best fit for each gas species. The values for h obtained in this way were all within 13% of the average value $h = 1.61 \mu\text{m}$ and are in line with the manufacturer's nominal value $1.5 \pm 0.5 \mu\text{m}$. Ideally the parameter h chosen by the fitting procedure would be independent of gas species and this is the case here to within a few per cent of the average. The values for η and M used as inputs to equation (17e) and the resulting values for h are included in table 1.

After the initial fitting of h shown in table 1 for each gas, h was fixed at its average value ($1.61 \mu\text{m}$) for the four gases. The gauge and absolute modes shown in figures 6(a)–6(d) are results with $h = 1.61 \mu\text{m}$. In the above analysis we have assumed a perfect piston and cylinder so that the annular width h was independent of z .

As can be seen in figure 6 the model described above by equation (17e) does reasonably well in fitting Γ for the piston and cylinder operating in the absolute mode for all four gases (N_2 , He, SF_6 and H_2) used in the present investigation and the model fits reasonably well in the gauge mode for all four gases except for H_2 at low pressure. The model also predicts the pronounced roll-off shown by the data for small applied pressures in the absolute mode.

The model in principle contains no free parameters although at present h is adjusted to optimize the fit to the data (it could be measured and eliminated as a free parameter). Independent fall rate measurements are sometimes used to determine h . In the present case this method yielded the value $h \approx 2.0 \mu\text{m}$ which is significantly higher than the value obtained by the spin time method. Since the fall rate method is very sensitive to gas volume changes with temperature and since the gauge was not thermostated we prefer the value of h obtained by fitting the model to measured values of Γ

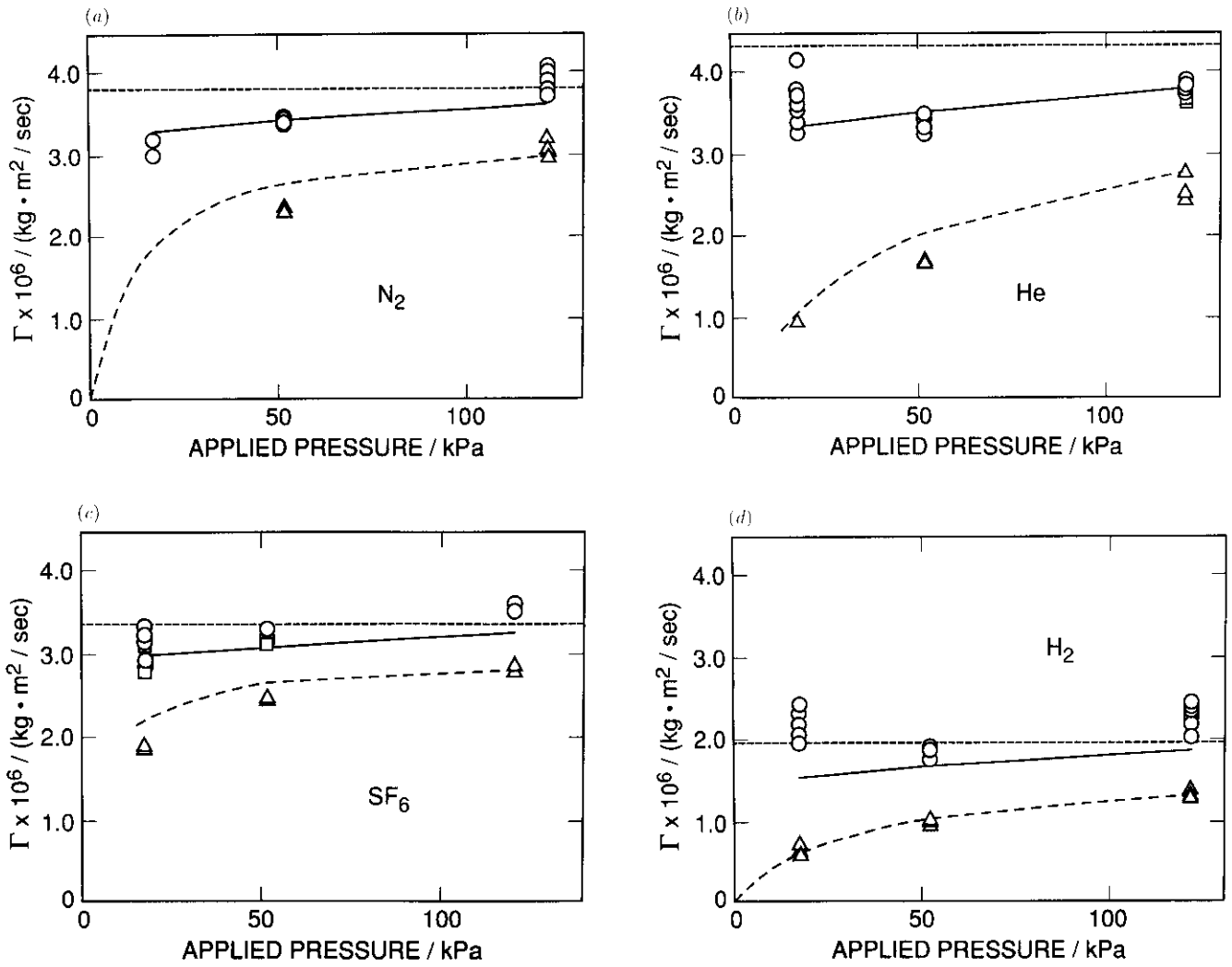


Figure 6. (a) The torque coefficient $\Gamma = \Gamma_{an} + \Gamma_s$ for N_2 as measured under various conditions as described in the text against differential pressure ($P_1 - P_0$). The full line indicates calculated values (present model) for the gauge mode. The broken curve indicates calculated values (present model) for the absolute mode. A simple viscous flow model would give a constant value for Γ independent of pressure (dotted line). Circles indicate measured values in the gauge mode; triangles indicate measured values in the absolute mode. (b) The torque coefficient $\Gamma = \Gamma_{an} + \Gamma_s$ for He as measured under various conditions as described in the text against differential pressure ($P_1 - P_0$). Notation is as in part (a) and squares indicate measured values in intermediate mode. (c) The torque coefficient $\Gamma = \Gamma_{an} + \Gamma_s$ for SF_6 as measured under various conditions as described in the text against differential pressure ($P_1 - P_0$). Notation is as in part (a) and squares indicate measured values in intermediate mode. (d) The torque coefficient $\Gamma = \Gamma_{an} + \Gamma_s$ for H_2 as measured under various conditions as described in the text against differential pressure ($P_1 - P_0$). Notation is as in part (a).

Table 1.

Gas species	Viscosity η ($10^{-6} \text{ kg m}^{-1} \text{ s}^{-1}$)	Molecular weight	Molecular mass M (10^{-27} kg)	Fitted parameter h (μm)
N_2	17.86 ^a	28	46.7	1.73
He	20.5 ^b	4	6.68	1.68
SF_6	15.34 ^c	146	243.8	1.61
H_2	8.45 ^d	2	3.34	1.42
				Av $\langle 1.61 \rangle$

^a See Hirschfelder *et al* [22].

^b See Chapman and Cowling [23]; table 13 extrapolated to 300 K.

^c See Kestin *et al* [24].

^d See Chapman and Cowling [23]; table 11 extrapolated to 300 K.

from the four gases. A possible explanation might be an asymmetry in the clearance between the pistons and cylinder, which would tend to decrease the value of h obtained by the rotational measurements and would tend to increase the value of h obtained by fall rate measurements. Other possible explanations for the discrepancy need to be explored in the future but are beyond the scope of this paper.

Although a combined species and mode change can produce large changes in Γ , a correspondingly large change in the generated pressure (or effective area) is not indicated by present theory, which is influenced by vertical rather than circumferential forces exerted by the gas in the annulus. Rather the theory [20], which covers only two limiting cases, is species independent and only weakly mode dependent. For the gauge used in the present measurements this limited theory would indicate that a change of less than 2 ppm in the effective area is expected when the mode is changed from gauge to absolute. Published measurements [3] on similar gauges indicate larger species effects of the order of 4 ppm. Other measurements [4] on different types of gauge indicate even larger mode and species effects of the order of 25 ppm. A definitive theory that can explain this discrepancy between theory and experiment has not yet been developed. As noted in the appendix equation (2b) assumes that molecules leaving a surface do so on average in a direction perpendicular to the surface with a frame of reference attached to that surface. Other models [21] that allow for specular reflections of molecules from surfaces might allow changes in the effective area large enough to cover the discrepancy between present theory and experiment. The upper bound on this effect would be of the order h/R which for the piston and cylinder used in the present measurement is ≈ 160 ppm.

5. Summary

Spin times were measured in a low-pressure pneumatic dead weight piston gauge for four gases He, H₂, N₂, and SF₆. Significant differences were observed between the different species of gas (H₂ and He for example) and even larger differences were observed between gauge and absolute modes of operation for the same gas (He for example). These differences were interpreted with a model for the momentum transfer function which depends on the pressure profile due to the gas in the annular space. This momentum transfer function bridges the transition region between viscous and molecular flow where the physics is better known and this function gives good agreement with measured values of the rotational torque coefficient when integrated over the annular region. The implications that the present results have for the determination of the effective area of this and other piston gauges have not yet been worked out. However the importance of the pressure profile in the annular region of a gas piston gauge in influencing the rotational behaviour of the gauge is clearly suggested.

Acknowledgments

This work has been supported by the US Air Force under contract CCG-910A038, Task 319 and by the NIST Office of Physical Measurements Services. JWS acknowledges very helpful discussions with Mike Moldover, Rich Kayser, Pat Looney, Ray Mountain and Asoka Ratnam. JWS also thanks Verne Bean for critical readings of the manuscript.

Appendix

1. Viscous flow regime

The velocity $v_\phi(r)$ of a fluid element in the azimuthal direction inside the annular region for a piston of radius R_1 rotating with angular velocity Ω inside a non-rotating cylinder of radius R_2 with radial clearance $h = R_2 - R_1$ is [6]

$$v_\phi(r) = \frac{\Omega R_1^2}{R_2^2 - R_1^2} \left(-r + \frac{R_2^2}{r} \right).$$

The drag force F_ϕ on the piston in the azimuthal direction is

$$F_\phi = 2\pi R_1 L \eta \left. \frac{dv}{dr} \right|_{R_1},$$

where L is the length, $2\pi R_1 L$ is the area of overlap between the piston and cylinder and η is the viscosity of the fluid. Evaluating $d_\phi/dr(r)|_{R_1}$ one obtains

$$\begin{aligned} F_\phi &= 2\pi R_1 L \eta \frac{\Omega}{R_2^2 - R_1^2} (-R_1^2 - R_2^2) \\ &= 2\pi R_1 L \eta \frac{\Omega}{2R_1 h + h^2} (-2R_1^2 - 2R_1 h - h^2). \end{aligned}$$

Since in the present case $h/R_1 \ll 1$, one obtains

$$F_\phi \simeq -2\pi R_1^2 L \eta \frac{\Omega}{h}.$$

The drag torque is then

$$\begin{aligned} R_1 F_\phi &\simeq -2\pi R_1^3 L \eta \frac{\Omega}{h} \\ &\simeq -\Gamma \Omega \end{aligned}$$

where the coefficient Γ is defined to be $(2\pi R_1^3 L \eta/h)$. This is equation (2a) in the text

$$\Gamma = R_1^2 \eta A/h$$

where A is the piston-cylinder overlap area $2\pi R_1 L$.

2. Collisionless flow regime

A piston with angular velocity Ω is assumed to rotate inside a stationary cylinder with mean radial clearance much less than the mean free path, and the change in angular momentum of the piston ($I\Delta\Omega$) due to the addition of one molecule with mass M that sticks

momentarily to the piston and then leaves is considered. It is further assumed that on average the molecules will arrive with only a radial component of velocity in the laboratory frame of reference and that the molecule leaves the piston on average in a direction perpendicular to the surface of the piston in the piston's rotating frame of reference. The average angular momentum change of the piston per event is then

$$I\Delta\Omega_1 = -MR_1^2\Omega.$$

The number of such events per unit time per unit surface area of the piston is

$$(n/2)\langle |v_r| \rangle =$$

$$\frac{n}{2} \int_0^\infty v_r \exp(-Mv_r^2/2kT) dv_r \Big/ \int_0^\infty \exp(-Mv_r^2/2kT) dv_r,$$

where n is the number of molecules per unit volume, v_r is the radial component of molecular velocity, M is the molecular mass, k is Boltzmann's constant and T is the thermodynamic temperature. The factor of $\frac{1}{2}$ is included because only half of the molecules surrounding the piston are moving toward the piston, the other half have already imparted their momentum to the piston and are moving away. Evaluating the integrals one obtains

$$\begin{aligned} \frac{n}{2} \langle |v_r| \rangle &= \frac{n}{2} \left(\frac{2kT}{\pi M} \right)^{1/2} \\ &= \frac{n \bar{c}}{2} \end{aligned}$$

where the mean molecular speed $\bar{c} = (8kT/M\pi)^{1/2}$. The total change in angular momentum of the piston per unit time integrated over the piston-cylinder overlap area is then

$$I \frac{\Delta\Omega}{\Delta t} = -2\pi MR_1^3 L \frac{n \bar{c}}{2} \Omega.$$

Finally we take the simplest case $n = P/kT$ and substitute to obtain:

$$I \frac{\Delta\Omega}{\Delta t} = -2\pi MR_1^3 L \frac{P\bar{c}}{kT4} \Omega$$

and then define a torque coefficient, in this case

$$\Gamma = 2\pi MR_1^3 L \frac{P\bar{c}}{kT4}.$$

This is equation (2b) in the text.

References

[1] Welch B E, Guildner L A and Bean V E 1985 Factors affecting the precision of gas operated piston gauges at the part per million level *Adv. Test Meas.* **22** 303

[2] Davis R S and Welch B E 1988 Practical uncertainty limits to the mass determination of a piston-gauge weight *J. Res. NBS* **93** 565

[3] Welch B E, Edsinger R E, Bean V E and Ehrlich C D 1989 The reduction of uncertainties for absolute piston gauge pressure measurements in the atmospheric pressure range *J. Res. NIST* **94** 343

[4] Welch B E, Edsinger R E, Bean V E and Ehrlich C D 1989 Observations of gas species and mode of operation effects on effective areas of gas-operated piston gauges *High Pressure Metrology* ed G F Molinar (Bureau International des Poids et Mesures Monographie) **89/1** p 81

[5] Tilford C R, Hyland R W and Sheng Yi-tang 1989 Non-geometric dependencies of gas-operated piston gauge effective areas *High Pressure Metrology* ed G F Molinar (Bureau International des Poids et Mesures Monographies) **89/1** p 105

[6] Landau L P and Lifshitz E M 1959 *Fluid Mechanics* vol 6 (London: Pergamon) ch 11 p 60

[7] Tilford C *et al* 1990 Vacuum calibrations using the molecular drag gauge (unpublished)

[8] Zemansky M W 1968 *Heat and Thermodynamics* 5th edn (New York: McGraw-Hill) ch 6 pp 145-65

[9] Moldover M R and Kayser R F 1991 Private communication

[10] Reif F 1965 *Fundamentals of Statistical and Thermal Physics* (New York: McGraw-Hill) pp 475-7

[11] Dushman S 1962 *Scientific Foundations of Vacuum Technique* (New York: Wiley) ch 2 pp 80-117

[12] Fremery J K 1985 The spinning rotor gauge *J. Vac. Sci. Technol. A* **3** 1715

[13] Lamb H 1945 *Hydrodynamics* 1st American edn (New York: Dover) ch 11

[14] Dushman S 1962 *Scientific Foundations of Vacuum Technique* (New York: Wiley) (See discussion in section 2.3 and equation (2.22) on p 86)

[15] Landau L P and Lifshitz E M 1959 *Fluid Mechanics* vol 6 (New York: Pergamon) (See p 56 equation (17.5) and section 17 p 57 Prob. 1)

[16] Dushman S 1962 *Scientific Foundations of Vacuum Technique* (New York: Wiley) p 87 (equation 2.25)

[17] Landau L P and Lifshitz E M 1981 *Physical Kinetics* (New York: Pergamon) vol 10 (section 15, Prob. 8)

[18] Bass A H 1978 Analysis of mechanical pressure generation *J. Phys. E: Sci. Instrum.* **11** 682

[19] Ratnam B A 1990 Patent applied for

[20] Dadson R S, Lewis S L and Peggs G N 1982 *The Pressure Balance—Theory and Practice* (London: NPL) p 246 equation (238), p 248 equation (245)

[21] Dushman S 1962 *Scientific Foundations of Vacuum Technique* (New York: Wiley) ch 1, section 1.8, p 35 1.109

[22] Hirschfelder J O, Curtiss C F and Bird R B 1954 *Molecular Theory of Gases and Liquids* (New York: Wiley) Table 8.4-2

[23] Chapman S and Cowling T G 1970 *The Mathematical Theory of Non-Uniform Gases* 3rd edn (Cambridge: Cambridge University Press)

[24] Kestin J, Khalifa H E, Ro S T and Wakeham W A 1977 *Physica* **88A** 242